

DTIC FILE COPY

Department of Mechanical and
Industrial Engineering
University of Illinois at
Urbana-Champaign
Urbana, IL 61801



2

AFOSR-TR- 90 - 0 4 4 9

**RESEARCH EQUIPMENT
PURCHASED UNDER URIP
GRANT AFOSR-86-0257**

AD-A221 371

Prepared by:

Dr. Herman Krier
Tel: (217)333-0529

Prepared for:

Air Force Office of Scientific Research
Attn: Dr. Mitat A. Birkan, Program Manager
AFOSR/NA
Bolling Air Force Base
Washington, D.C. 20332-6448
Tel: (202)767-4938

May 1989

DTIC
ELECTE
MAY 11 1990
S E D

DISTRIBUTION STATEMENT A
Approved for public release;
Distribution Unlimited

FINAL TECHNICAL REPORT

90 05 10 180

FINAL TECHNICAL REPORT

RESEARCH EQUIPMENT PURCHASED
UNDER URIP, GRANT AFOSR-86-0257

Prepared by:

Dr. Herman Krier
Principal Investigator
Department of Mechanical and Industrial Engineering
University of Illinois at Urbana-Champaign
(217)333-0529

Prepared for:

Air Force Office of Scientific Research
Attn: Dr. Mitat A. Birkan, Program Manager
AFOSR/NA
Bolling Air Force Base
Washington, D.C. 20332-6448
(202)767-4938



May 1989

Accession For	
NTIS GRA&I	<input checked="" type="checkbox"/>
DTIC TAB	<input type="checkbox"/>
Unannounced	<input type="checkbox"/>
Justification	
By _____	
Distribution/ _____	
Availability Codes	
Dist	Avail and/or Special
A-1	

REPORT DOCUMENTATION PAGE

Form Approved OMB No. 0704-0188

1. REPORT SECURITY CLASSIFICATION Unclassified		1b. RESTRICTIVE MARKINGS	
2. SECURITY CLASSIFICATION AUTHORITY		3. DISTRIBUTION / AVAILABILITY OF REPORT Approved for public release; distribution is unlimited	
4. DECLASSIFICATION / DOWNGRADING SCHEDULE		5. MONITORING ORGANIZATION REPORT NUMBER(S) AFOSR-TR-90-0449	

6a. NAME OF PERFORMING ORGANIZATION University of Illinois at Urbana-Champaign	6b. OFFICE SYMBOL (if applicable) UIUC	7a. NAME OF MONITORING ORGANIZATION AFOSR/NA	
--	--	---	--

8. ADDRESS (City, State, and ZIP Code) Dept. of Mechanical & Industrial Engineering 10 MEB; 1206 West Green Street (MC-244) Urbana, IL 61801		7b. ADDRESS (City, State, and ZIP Code) Building 410, Bolling AFB DC 20332-6448	
---	--	---	--

9a. NAME OF FUNDING / SPONSORING ORGANIZATION AFOSR/NA	8b. OFFICE SYMBOL (if applicable) NA	9. PROCUREMENT INSTRUMENT IDENTIFICATION NUMBER AFOSR-86-0257	
---	--	--	--

10. SOURCE OF FUNDING NUMBERS			
PROGRAM ELEMENT NO. 61102F	PROJECT NO. 2308	TASK NO. A1	WORK UNIT ACCESSION NO.

11. TITLE (Include Security Classification)
RESEARCH EQUIPMENT PURCHASED FOR LASER PROPULSION UNDER A URIP GRANT (AFOSR)

12. PERSONAL AUTHOR(S)
Herman Krier

13a. TYPE OF REPORT Final Technical	13b. TIME COVERED FROM: 01/86 TO 05/89	14. DATE OF REPORT (Year, Month, Day) May 22, 1989	15. PAGE COUNT 42
--	---	---	----------------------

16. SUPPLEMENTARY NOTATION

17. COSATI CODES			18. SUBJECT TERMS (Continue on reverse if necessary and identify by block number)
FIELD	GROUP	SUB-GROUP	

19. ABSTRACT (Continue on reverse if necessary and identify by block number)

Through AFOSR, as part of the University Research Instrumentation Program, the Department of Mechanical and Industrial Engineering of the University of Illinois was awarded the funds to purchase equipment in support of research dealing with high temperature thermodynamics, plasma formation, and laser-gas interaction. AFOSR has been supporting research under a separate grant, a program dealing with Beamed Energy (Laser) Rocket Propulsion.

This report summarizes research instrumentation purchased on this grant program. Information on Digital Imaging and Laser Induced Fluorescence is given. The equipment includes: Excimer Laser; Dye Laser; Imaging Optics and support equipment. The report also summarizes research capabilities now possible in non-equilibrium laser-sustained plasmas. (J25)

20. DISTRIBUTION / AVAILABILITY OF ABSTRACT <input checked="" type="checkbox"/> UNCLASSIFIED/UNLIMITED <input checked="" type="checkbox"/> SAME AS RPT. <input checked="" type="checkbox"/> DTIC USERS		21. ABSTRACT SECURITY CLASSIFICATION Unclassified	
22a. NAME OF RESPONSIBLE INDIVIDUAL Dr Mitat Birkan		22b. TELEPHONE (Include Area Code) (202) 767-4938	22c. OFFICE SYMBOL AFOSR/NA

**RESEARCH EQUIPMENT PURCHASED
UNDER URIP, GRANT AFOSR 86-0257**

INTRODUCTION

Through AFOSR, as part of the University Research Instrumentation Program the Department of Mechanical and Industrial Engineering of the University of Illinois was awarded the funds to purchase equipment in support of research dealing with high temperature thermodynamics, plasma formation, and laser-gas interaction. AFOSR has been supporting research under a separate grant, a program dealing with Beamed Energy (Laser) Rocket Propulsion.

We requested and were awarded the equipment listed in Table I. The estimated cost per item is shown. The total amount of the award was \$184,450.

It has turned out that Professor Herman Krier and Professor John P. Renie were awarded another URIP grant, through the Office of Naval research (ONR) for permanent equipment in support of DoD research on Supersonic Mixing and Combustion for SCRAMJET Propulsion. We purchased, under the ONR grant, almost all of the items dealing with the Digital Imaging System, i.e., items number 4 - 9 shown in Table I.

**TABLE I: PERMANENT EQUIPMENT
ORIGINALLY REQUESTED/AWARDED**

No.	ITEM/DESCRIPTION	AMOUNT
1.	Tunable Dye Laser	\$ 28,000.
2.	Beamsplitting and Steering Optics	2,000.
3.	Frequency Doubler	4,000.
4.	Minicomputer	60,000.
5.	Image Acquisition Subsystem	32,000.
6.	Intensifier Subsystem	45,000.
7.	Gated Power Supply	5,000.
8.	Fortran Compiler	5,000.
9.	Cabinets and Tables	3,450.
TOTAL =		\$184,450.

Appendix A is a description of that instrumentation which is operational and shared between the researcher's supported by AFOSR and ONR.

PERMANENT EQUIPMENT
PURCHASED UNDER THIS GRANT

In order to measure extreme temperatures in both the Laser-Plasma Research (AFOSR) and the Supersonic Combustion Research (ONR) the non-intrusive technique of Laser-Induced Fluorescence (LIF) will be used. Appendix B is a summary of that technology, and the instrumentation usually required.

A major portion of the funds expended to date therefore are lasers required to perform LIF. (Authorization by AFOSR had been given to make these changes.)

Just as important, these URIP funds allowed for the purchase of optical equipment and accessories which provided for the diagnostic analysis of high temperature argon and hydrogen plasmas.

Table II is a summary of the equipment purchased on this contract.

TABLE II: EQUIPMENT PURCHASED

No.	ITEM/DESCRIPTION	AMOUNT	P.O. #
1.	Tunable Dye Laser (Lumonics)	41,200.00	JR38064
2.	Excimer Laser (Questex Inc.)	49,900.00	JR36099
3.	Optical Table System (Oriel Corp.)	4,405.71	JR39731
4.	Digital Delay Generator (Stanford Research Corp.)	3,660.90	JR39691
5.	Boxcar Signal Averager System (Stanford Research Corp.)	12,328.75	JR45323
6.	Optical Lenses [Zinc Selenide] (Two-Six Inc.)	8,728.60 2,646.79	JR35740 JR50899
7.	4-Watt Plasma Tube (Cooper Lasersonics)	8,845.13	JR99087
8.	Linear Positioning Stages (Aerotech Inc.)	18,869.00	JR92225
9.	Optical Breadboard (Newport Corp.)	2,691.94	JR90218
10.	Optical Tables (Oriel Corp.)	5,959.53	JR57419
11.	Pressure Submodule (Pressure Systems)	1,262.46	JR59068
12.	FX86E Printer (MMT)	306.00	JRD8084
13.	Optical Table (Oriel Corp.)	2,643.58	JR90742
14.	Electronic Pressure Scanner (Pressure Systems)	4,871.98	JR57230
15.	Electronic Components and Analyzer (UIUC Central Stores)	2,814.00	GS129083
16.	Copier [Optical] (CDS Systems)	207.43	JR473153
17.	Optical Benches (Newport Corp.)	3,079.60	JR92238
18.	Gas Detector for H ₂ (Macurco)	433.75	JRD2891
19.	Control Valves for H ₂ Gas (Enpro)	4,248.45	JR88898
20.	H ₂ Exhaust Facility Equipment and Installation (1988-89)	5,316.40	Dept. Transfer
Total =		\$184,450.00	

II. CAPABILITIES TO PERFORM RESEARCH
ON
NON-LOCAL THERMODYNAMIC EQUILIBRIUM
IN
LASER SUSTAINED PLASMAS

Table of Contents

I. Introduction	1
A. Objectives and Background	1
B. Previous Experiments.....	1
C. Local Thermodynamic Equilibrium.....	2
D. Plasma Diagnostics.....	4
E. Modeling Implications	6
F. Literature Review.....	6
II. Laser Sustained Plasma Physics.....	9
A. Local Thermodynamic Equilibrium.....	9
B. Basic LTE Criteria.....	11
1. Kinetic Temperature	11
2. Excited State and Ionizational Equilibrium.....	12
3. Maxwellian Electron Velocity Distribution.....	14
C. Laser Absorption and Radiative Emission in LSP's.....	14
1. Absorption Coefficients.....	15
2. Emission Coefficient	17
III. Experimental and Analytical Techniques.....	18
A. Experimental Technique	18
1. Electron Number Density	18
2. Absolute Line Intensities.....	19
B. Analytical Technique	20
C. Proposed Experimental Agenda.....	21
IV. References.....	22

I. Introduction

A. Objectives and Background

In our proposed research, a laser sustained plasma (LSP) is being studied with application to rocket propulsion in mind. Defining the thermodynamic state, be it an equilibrium state or otherwise, is a key issue for the basic physical understanding and performance evaluation of plasmas in this regard. This research aims to provide more accurate LSP diagnostics and to better evaluate their performance based on these diagnostics. LSP operating conditions will be defined for which local thermodynamic equilibrium can be guaranteed so that equilibrium numerical modeling can be undertaken with full confidence.

The so called laser propulsion system was first proposed by Kantrowitz [1,2]. Such a system would rely on a remotely based laser, either earth-bound or in low earth orbit, as its power source rather than conventional on-board chemical or electrical systems. The high power beam (~10 MW) would be aimed at a spacecraft in low earth orbit and collected by the craft's optical system. The power would then be focussed and absorbed in a flow chamber by a gas plasma, most likely hydrogen. The laser energy absorbed by the plasma would be converted (by convection and conduction) into thermal energy of the gas, and into radiation lost by the gas. The gas thus heated would then be accelerated out of a conventional rocket nozzle to provide thrust. The advantages of this system are numerous and a review of the early work concerning laser propulsion is given by Glumb and Krier [3].

B. Previous Experiments

The bulk of the experimental research performed at the UIUC has been concerned with measuring and optimizing LSP global absorption and thermal conversion efficiency [4,5,6,7]. Global absorption is the fraction of incident laser power absorbed by the plasma, whereas thermal conversion efficiency is the fraction retained by the gas as useful thermal energy. The balance is lost as optically thin radiation. In the laboratory laser power, gas mass flux, gas pressure, gas mixture, and beam focussing geometry can all be varied in the optimization effort.

In these experiments a 10 kW cw CO₂ laser has been used to produce laser-sustained argon plasmas. Argon has been used as a safe substitute for hydrogen and can be easily maintained as a

plasma with the available laser power. In addition such properties as laser absorption coefficient and radiative emission coefficient are similar for argon and hydrogen so that the experiments have had practical relevance. Although the available power level is several orders of magnitude less than that be required in practice, the work has been successful in that thermal conversion efficiency has been measured at values greater than 50 %, which is considered the feasibility limit for the laser propulsion concept. At certain operating conditions an argon plasma has been shown to absorb nearly 100 % of the incident laser power, which is vital for rocket considerations.

Figure 1 shows some of the results of pure argon plasma experiments [6]. The increase in pressure (and thus absorption coefficient) allowed for a greater mass flux to be applied without causing instability and plasma "blowout". Nearly all of the incident radiation is absorbed, and thermal efficiency is shown to be optimized at a certain mass flux for this laser power. The results shown in Figure 2 indicate the advantage of operating the LSP with a mixture of argon and helium [7]. Although the much greater ionization potential of helium limits the number of free electrons and thus global absorption, the greater overall thermal conductivity of this mixture plasma enhances that particular energy loss mechanism and reduces the energy loss due to radiation. The thermal conductivity of hydrogen is also quite high, indicating what might be expected in future experiments using pure hydrogen or argon/hydrogen mixtures.

The previous two figures point up the importance of absorption and radiation processes in the LSP. If the plasma is absorbing nearly all of the incident energy, but only converting half of that to thermal energy of the exhaust gas, the rest must be lost in radiation to the chamber walls. Obviously it is important to understand the nature of the radiation losses, how they are affected by the thermodynamic state of the plasma, and how they can be minimized.

C. Local Thermodynamic Equilibrium

In determining the thermodynamic state of the plasma, it is important to understand the concept of plasma temperature and the partitioning of energy. The energy content of the plasma gas is taken up by various modes. These include the kinetic energy of the free electrons and the heavy particles (neutral atoms and ions), the ionization energy of the ions, and the electronic excitation of the heavy particles. To a good approximation, the distribution of the energy in each

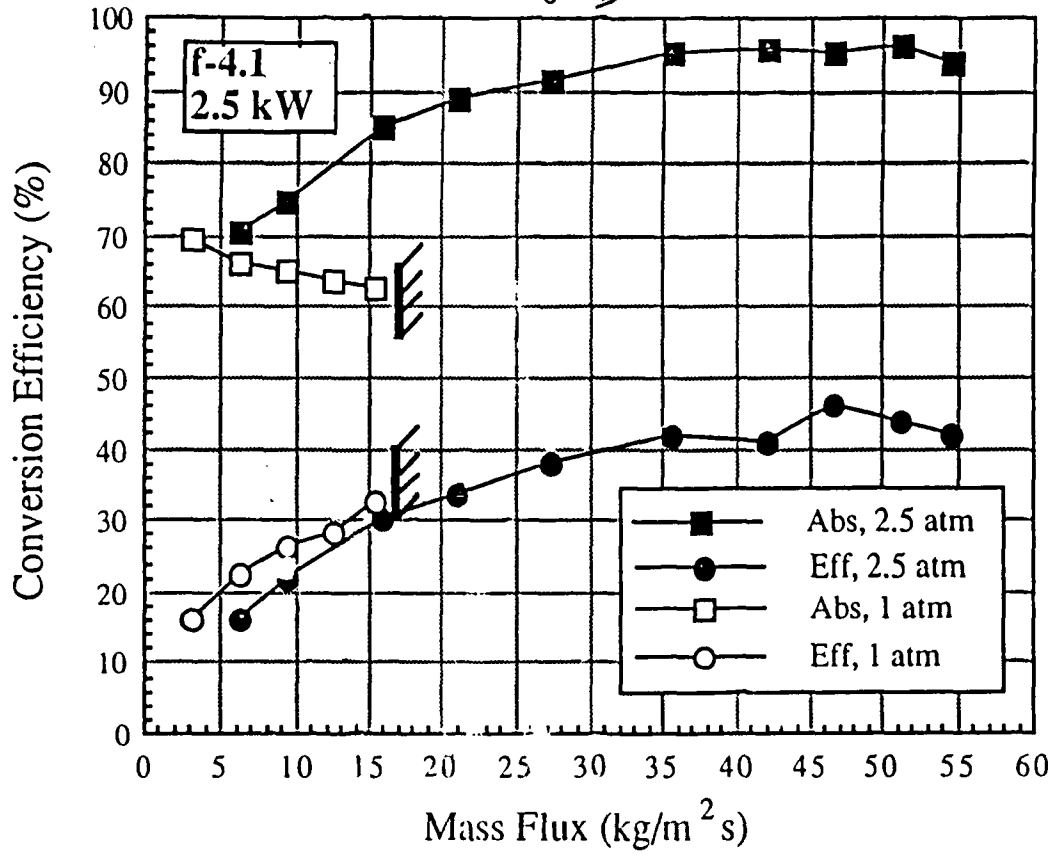


Figure 1 Comparison of global absorption and thermal efficiency for *f*-4.1, 2.5 kW LSP's at 1 atm. and 2.5 atm. gas pressure. Walls superimposed on figure denote 1 atm. stability mass flux limit. Note peak in thermal efficiency of 46% for 2.5 atm. LSP's.

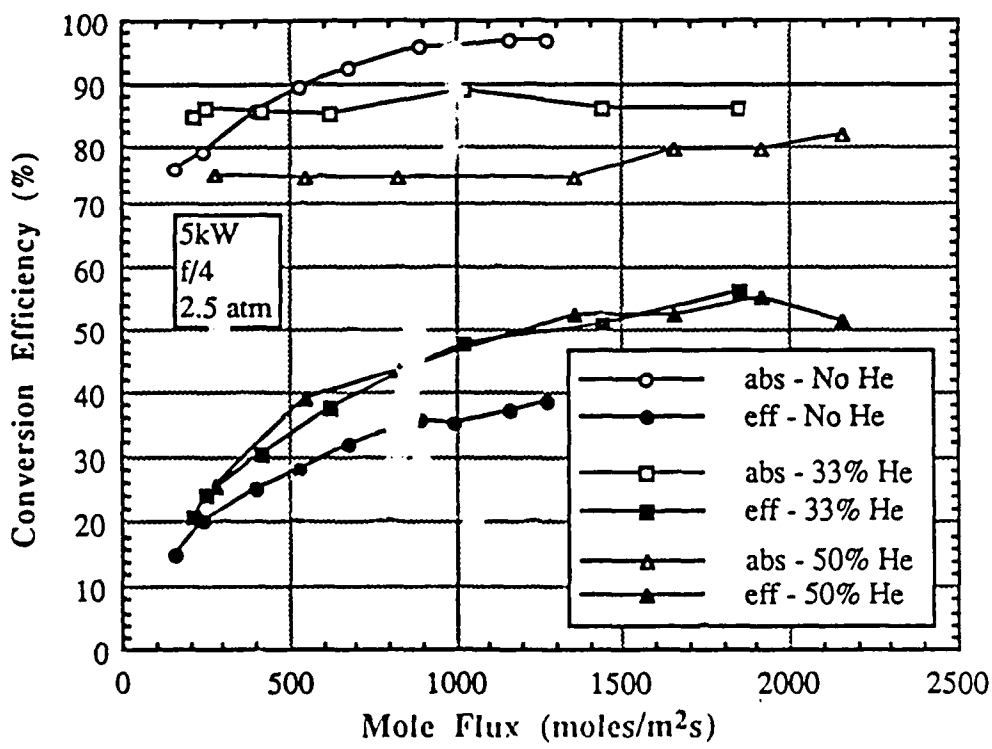


Figure 2 Comparison of global absorption and thermal efficiency for helium-argon mixture LSP's at 5 kW, 2.5 atmospheres and *f*/4.1 beam geometry. Results for pure argon, 33% helium by volume, and 50% helium by volume are presented.

of these modes can be characterized by a temperature parameter associated with Maxwell-Boltzmann statistics [8]. The degree of ionization in the plasma can be similarly characterized by temperature (through the Saha equation). If the plasma is in thermodynamic equilibrium then the thermodynamic state is completely determined by the values of any two properties such as pressure and temperature [9, p.5]. In thermodynamic equilibrium Boltzmann's formula for the distribution of excited electronic states, Maxwell's law for the distribution of particles velocities (energies), and Saha's equation describing the plasma composition are all associated with the same temperature parameter.

Strictly speaking, there can be no gradients of temperature or density in order for complete thermodynamic equilibrium to hold. Because gradients practically always exist in laboratory plasmas, complete thermodynamic equilibrium is almost never observed. Radiation escaping from the plasma and diffusion of charged particles toward its boundaries are two of the causes for the breakdown of equilibrium. However, if the processes which tend to maintain equilibrium (collisions between plasma particles) are intense enough, then thermodynamic equilibrium can be maintained locally [9]. Thus temperature and density are dependent upon location in the plasma, but the equations of thermodynamic equilibrium mentioned in the above paragraph hold at the local temperature. This situation is known as local thermodynamic equilibrium (LTE).

D. Plasma Diagnostics

As mentioned previously the past LSP research has been directed toward measuring their performance in terms of global laser absorption and thermal conversion efficiency. In order to better understand these results on a physical level it is important to be able to measure temperature and densities inside the plasma. Absorption of laser energy and radiation from the plasma at each point in the plasma will depend on these plasma conditions, thus enabling an understanding of the global results on a local level. The existence of LTE in the plasma greatly simplifies the diagnostic techniques required to fully describe the thermodynamic state. It is for this reason that the LTE assumption has been made in most LSP investigations [10-16]. There has been somewhat loose justification for this assumption based on electron number density considerations, but the existence of tremendous gradients of temperature and density, radiation losses, diffusion of charged particles,

and an intense external electric field (laser beam) lead to the current belief that LTE does not exist in laboratory LSP's in general.

Without an assumption of LTE, plasma diagnostics must be used which are not based on assuming the usual partitioning of energy in the system. A common LTE technique involves taking the ratio of line radiation intensity to the adjacent continuum radiation intensity and relating that quantity to electron temperature. Obviously if the excited state distribution, which gives rise to the line radiation, is not in equilibrium with the electron energy distribution this technique will not give meaningful results. Eddy gives an excellent review of the various LTE plasma diagnostic techniques and the problems which may arise in their application to a non-LTE situation [17].

In this proposed research, diagnostic techniques will be applied which are independent of the LTE assumption. These techniques follow those of Eddy and incorporate both direct spectroscopic measurements and analytic solution techniques [18,19]. Electron number density can be determined through either a spectral line broadening measurement or a measurement of continuum emission. The upper level excited state distribution temperature and state populations can be determined from a measurement of spectral line intensities. Other relevant parameters such as electron and heavy particle kinetic temperatures, atomic number density, and the total excitation temperature (relating the ground state to the highest excited state), can be calculated through an iterative simultaneous solution of the appropriate analytical expressions. These experimental techniques will be described more thoroughly in a later section of this proposal.

In all the studies mentioned above of the types of LSP's considered here (forced convection regime for the laser propulsion application) [12-15], local laser absorption and radiative emission coefficients were taken to be functions of the plasma electron temperature only, at a given pressure. The temperature used was the one found through the use of LTE diagnostics or single temperature modeling. It is a goal of this proposed research to arrive at better values for absorption and emission coefficient based on the measured or calculated value of number densities and temperatures, using the techniques described in the preceding paragraph. It is expected that this will lead to a more fundamental understanding of the laser energy conversion process and to more accurate determinations of global absorption and thermal conversion efficiency.

E. Modeling Implications

A major goal of the ongoing research has been to predict LSP performance trends (global absorption and thermal conversion efficiency) at the conditions expected in an actual laser thruster (high laser power and mass flux, for example). To this end a computer program has been developed by Eguiguren which models the two dimensional flow in the plasma chamber [7]. This model is similar to the one developed earlier by Jeng and Keefer [10]. Although Eguiguren's model has been very successful at matching the trends in the experimental results, it always tends to overpredict thermal efficiency. Figure 3 is a comparison of numerical and experimental results for pure argon plasmas. The numerical prediction of thermal efficiency is an average of 18 % higher than the efficiency measured with thermocouples in the chamber exhaust ports.

All the computer simulations of LSP's reported assume a single temperature in the energy equation and use LTE property values. In order to have confidence in using a computer model for operating conditions not attainable in the laboratory, it must be known for certain whether the observed differences from the experimental data are due to non-LTE effects. In the event that non-LTE is shown to be a dominant factor for certain LSP experimental conditions, either a model must be developed which takes these effects into account, or care must be taken to rely upon the current models only when LTE can be assured. The results of this proposed research will provide guidance in this regard.

F. Literature Review

There has been no record found in the literature of non-LTE diagnostics performed on continuously maintained laser produced plasmas. There are several reports of LSP diagnostics performed which make claims concerning LTE. Generalov et al. [10] used Stark broadening of the $H\beta$ line to calculate electron number density in argon and xenon LSP's, and the Saha equation was used to calculate temperature assuming equilibrium. An approximate calculation of the maximum deviation of the electron temperature from the heavy particle temperature resulted in only a 6% deviation for argon based on 100 W input laser power. The conclusion was that the LSP is in LTE to a first approximation. In this experiment, however, no attempt was made to determine the excitation temperature or to resolve the electron number density and temperature spatially. In

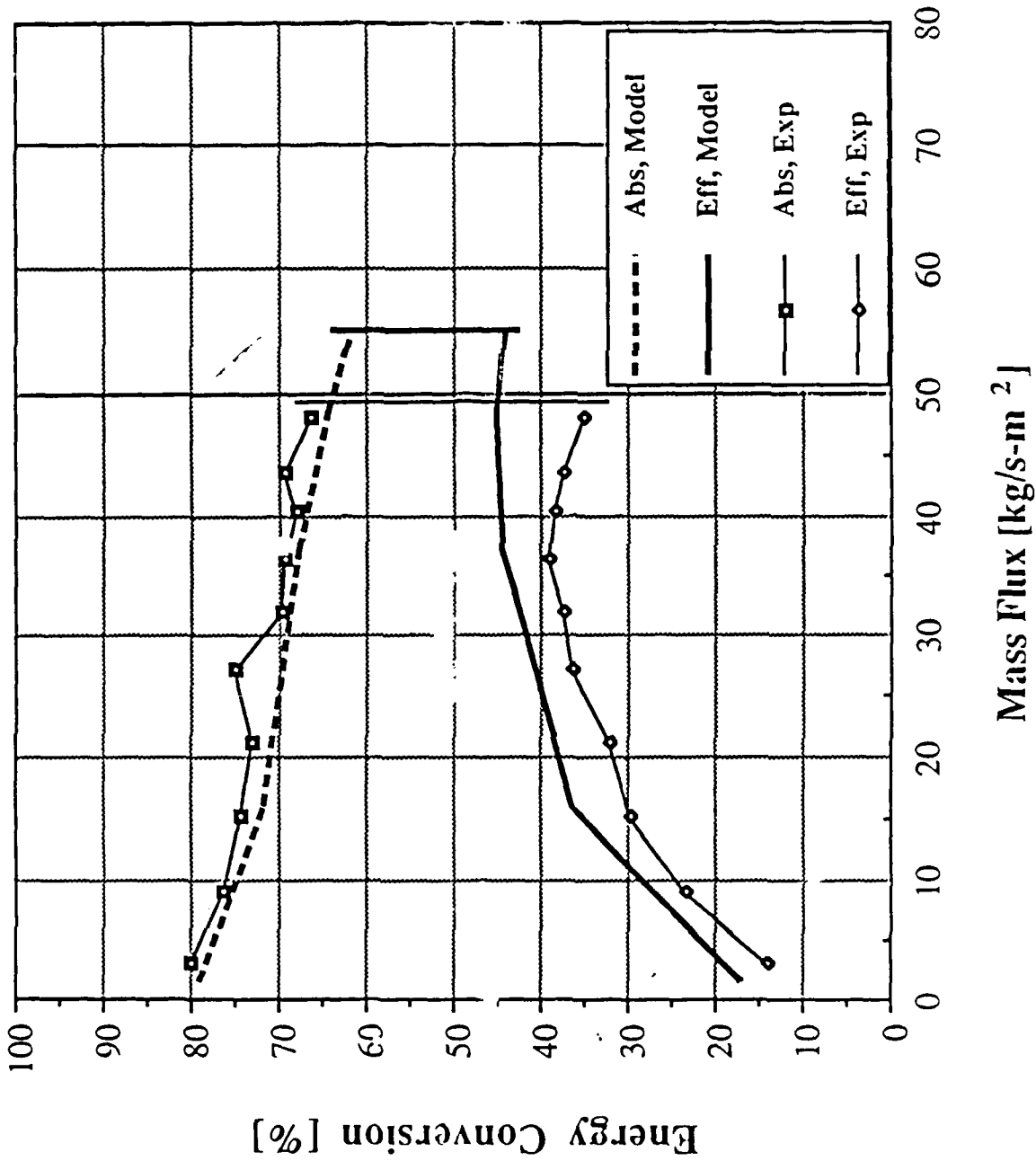


Figure 3 Model vs. experiment energy conversion comparison for an argon plasma at f/4 and 5 kW conditions.

another study of air LSP's Keefer et al. [20] used the Fowler-Milne and absolute line intensity techniques to measure plasma temperature. Both of these techniques require that LTE exist to retain accuracy, and although the results are in agreement internally, LTE cannot be concluded from this experiment. Keefer states that the presence of anomalous excited rotational structures in the molecular nitrogen ion found near the plasma boundaries may be due to non-LTE processes. In a study of xenon LSP's Cremers et al. [21] measured electron number density via Stark broadening and temperature via the Saha equation (assuming equilibrium). A Boltzmann plot was made after adding 66% krypton and using the krypton relative line intensities. The Boltzmann temperature agreed well with the Saha temperature, but as stated by the authors, "The quality is not sufficient to indicate positively that the (Boltzmann) plot is linear." This along with no Abel inversion of the data, the comparison of two differently composed plasmas, and the assumption of equilibrium in the use of the Saha equation prevent a confirmation of LTE in these LSP's.

There are numerous reported investigations, both theoretical and experimental, of pulsed laser produced plasmas [22-24]. The enormous power of most laser pulses and the transient nature of the plasmas in these articles reduce the applicability of their results to this proposed research. In general it is concluded that LTE does not exist in these plasmas, except at superhigh-pressure [22]. Tonon et al. [23] concluded that electron and ion kinetic temperatures are the same in a plasma produced by a giant laser pulse on a solid target. This conclusion is based on a best fit of experimental data to theoretical analysis. Vorob'ev and Khomkin [24] performed a theoretical analysis of a continuous laser produced plasma near a metal surface. It was found that ionizational nonequilibrium existed for surface fluxes on the order of 10^6 W/cm².

A much larger amount of research has been done on plasmas produced in an electric arc [18,25-31]. There is general agreement that complete LTE does not exist in electric arc plasmas at pressures less than or equal to one atmosphere. Above one atmosphere conclusions vary as to the pressure at which LTE can be expected. Farmer and Haddad [25] state that above 1.4 atm. LTE existed in an argon arc based on evidence of a constant off-axis maximum in the emission coefficient. Bober and Tankin [26] suggest that an argon arc will not be in LTE until a pressure of 3 atm. This conclusion comes from an extrapolation of measured transition probabilities of an ArI

line to a pressure at which the probability becomes constant, indicating LTE. Eddy and Sedghinasab [18] show that in an argon arc with 1 % hydrogen the electron and heavy particle temperatures converge above 5 bar, but the upper level excitation temperature of argon atoms is still well above the electron temperature even at 10 bar. The pressure in a plasma relates directly to the electron number density, which is the key parameter in determining if LTE exists [32, p.148]. In this proposed research one goal is to determine the critical electron number density (pressure) for LTE as a function of the remaining operating conditions.

II. Laser Sustained Plasma Physics

A. Local Thermodynamic Equilibrium

In all plasmas in which complete thermodynamic equilibrium does not exist, the opposing collisional processes which tend to maintain equilibrium (ionization and recombination, excitation and deactivation) do not exactly counterbalance each other [9, p.10]. Local thermodynamic equilibrium (LTE) holds if at each point in the plasma these processes far outweigh the processes which lead to a departure from equilibrium. For example the collisional excitation and deactivation of a particular electronic state should compensate for the depletion of that state by the escape of radiation from the local plasma volume. Similarly the collisional rate of ionization should be many times higher than the rate of electron diffusion out of the local plasma volume.

Each of these collisional processes has associated with it a collision cross section, and the inelastic processes also have corresponding transition probabilities. These transition probabilities are a function of the density and energy of the electrons and are very important for evaluating the dominant plasma processes. The collisional transitions which are the most probable are the ones between adjacent energy levels [9, p.31], and the ionization transitions which are the most probable are those originating in a highly excited state [9, p.45].

Loss of plasma energy due to spontaneous emission can have a strong impact on the plasma energy balance. For a fixed upper level, the most probable transition is to the ground state. Transitions to the adjacent lower level and to the first excited state in the atom are about 1/2 as likely to occur spontaneously. All other transitions are even less likely. For a fixed lower level a

transition from the adjacent higher level is the most probable, and all other transitions are much less likely to occur spontaneously.[9, p.70].

As a rule radiative transition probabilities decrease and collisional transition probabilities increase as the energy level in question increases [9, p.119]. It is then reasonable to expect that there will be a group of excited levels adjacent to the continuum that are in Boltzmann equilibrium amongst themselves. In addition radiative processes in plasmas become more important with decreasing plasma electron density and collision frequency. A higher density, and therefore higher collision frequency, means that electronic transitions within the atomic system will be collision dominated in lower lying energy levels as well, and the Boltzmann distribution may hold completely if the electron number density is high enough. As mentioned in the previous section, the electron density at which the plasma state is determined solely by electron collisions is not known precisely for all cases.

A process which tends to break down equilibrium in inhomogeneous plasmas is the radiative transport of atomic excitation energy from one point in a plasma to another. This kind of energy transport is a sequence consisting of absorption of radiation and its reradiation by the excited atoms resulting in excited atoms that seem to move in space. Although considered an optically thick radiative process, excitation transport can have a nonequilibrium influence because the density and spatial distribution of excited atoms is altered and thus can effect the plasma properties and processes such as ionization and recombination.

In many cases the average distance between the sites of photon emission and absorption is much larger than the mean free paths of the plasma particles. This means that radiative excitation transport couples regions of the plasma which otherwise would not strongly interact. Due to the variation of absorption coefficient across a broadened line spectrum, the radiation emitted in these lines is attenuated more slowly than the familiar exponential decay of a pure frequency. As a result, excitation can be transported into a given plasma volume from remote regions of the plasma [9, p.88]. If this process is significant in LSP's, then there is the possibility that even at high electron number density the distribution of excited states will not follow a Boltzmann distribution, or that the distribution is not in equilibrium with the local free electrons.

B. Basic LTE Criteria

In general, external electromagnetic fields, the escape of radiation outside the plasma, gradients of physical quantities, and the finite rate of physical and chemical processes all work to destroy equilibrium in a plasma. Collisional processes, which lead to a redistribution of energy and momentum of the plasma particles, work to restore equilibrium. The criteria for determining if a plasma volume is in equilibrium requires comparing the efficiency of the processes working to destroy and restore equilibrium.

1. Kinetic Temperature

In this kind of nonequilibrium the electron kinetic temperature is not the same as the heavy particle kinetic temperature. It arises when an external field is applied to the plasma. The mobility of the electrons is much higher than that of the heavy particles, and so the bulk of the energy is transferred to the electrons. In other words the inverse bremsstrahlung (IB) laser absorption process increases the kinetic energy of the electrons much more than it does the heavy particles in the electron-photon-heavy particle three body collision.

Laser irradiance (W/m^2) can be expressed in terms of the amplitude of its electric field vector (V/m) by the following;

$$I = \frac{c \epsilon_0}{2} E_0^2$$

For a laser power of 5 kW giving a modest irradiance estimate of $10^8 W/m^2$ the electric field amplitude is $2.7 \times 10^5 V/m$. Griem [33, p.157] gives a criterion for kinetic equilibrium based on the amount of energy absorbed by the electrons and the amount transferred to the heavy particles through elastic collisions. The expression is given in terms of the external electric field strength;

$$E^2 \ll \left[5.5 \times 10^{-12} N_e \frac{E_H}{kT} \right]^2 \frac{m}{M}$$

E_H is the ionization potential of hydrogen (eV), N_e is the electron number density (cm^{-3}), kT is the average plasma electron energy (eV), m is the mass of the electron, and M is the mass of the heavy particle in question. For an equilibrium composition of argon at one atmosphere the maximum electron density at 16700 K is $\sim 2 \times 10^{17}$. The right hand side of this inequality is 1.5×10^9 for

these conditions and the criterion fails by at least two orders of magnitude. The situation is better for hydrogen but the electric field is still too strong by at least one order of magnitude. Therefore it is reasonable to expect kinetic nonequilibrium in LSP's particularly in the regions of laser beam propagation.

At higher temperatures inelastic collisions play a role in the steady state energy balance as will other electron energy loss mechanisms such as thermal conduction, radiation, and diffusion out of the plasma volume. These processes will ease the strictness of the above criterion, as will the presence of a molecular component in the plasma. With a molecular component the inelastic losses due to excitation of vibrational and rotational degrees of freedom become important and the effective energy transfer fraction can become many times larger than m/M thus enhancing the electron energy loss. This has been shown to be true even when molecules constitute only a small fraction of the total number of particles [9, p.115]. Even with these additional considerations the magnitude by which the above criterion failed for the laboratory LSP leads to the expectation of kinetic nonequilibrium.

2. Excited State and Ionization Equilibrium

For plasma diagnostics it is important to determine whether the atoms are distributed over the excited energy levels in accordance with a Boltzmann distribution at the electron temperature, and whether the electron density is given by the Saha equation at that same temperature. If these two situations hold, then the state of the plasma is greatly simplified and standard plasma diagnostic methods can be used.

LTE can be disturbed in a number of ways, the most important of which are, the escape of optically thin radiation, the diffusion of charged particles, and the optically thick transport of excitation energy. In general the breakdown of ionization equilibrium and the equilibrium excited state distribution are closely related.

A criterion stated by Griem [33, p.151] gives the electron number density required for a Boltzmann distribution to extend to the ground state of an atom. If this criterion is met, it is implied that the distribution of excited states and the extent of ionization are controlled by the electron kinetic temperature. The expression for critical electron number density is;

$$N_e \geq 9 \times 10^{17} \left[\frac{E_2}{E_H} \right]^3 \left[\frac{kT}{E_H} \right]^{\frac{1}{2}}$$

where E_2 is the energy of the first excited state. For argon at 18000 K this criterion is satisfied, but at 10000 K it fails, based on the equilibrium composition of argon at one atmosphere. Therefore it might be expected that the high temperature core of the LSP is in distribution and ionization equilibrium, but that the gas near the cooler plasma boundaries is not.

The above criterion assumes that there are no factors at work to destroy equilibrium other than the escape of optically thin line radiation. The situation is actually quite complex due to the entrapment of resonance radiation in the outer plasma regions which tends to enhance equilibrium, and the presence of steep gradients in temperature which tends to destroy equilibrium. Trapped resonance radiation reduces the overpopulation of the ground state, while steep gradients produce changes in plasma properties over distances shorter than the mean free path of an atom.

Diffusion of charged particles to the boundaries of the plasma volume is another important nonequilibrium factor. This process directly influences the ionization equilibrium by lowering the density of charged particles. In order to compensate for the resultant influx of neutral particles, ionization must exceed recombination.

Ionizational equilibrium can also be disturbed as a result of the escape of recombinational radiation. In this case there is a depletion in the number of free electrons which must be made up for by more intense collisional ionization. Line radiation also has an indirect effect on ionizational equilibrium. Since it is mainly excited atoms which are ionized, a decrease in the density of these atoms due to line radiation will decrease the number of ionization events and hence the density of charged particles. Similarly the diffusion of charged particles has an indirect effect on the distribution equilibrium. In this case (in the absence of radiation effects) ionization outweighs recombination, thus upward collisional transitions happen more often than downward collisional transitions.

The end result of the complex interaction of equilibrating and nonequilibrating processes is that it is not reasonable to rely on analytical expressions for the critical electron number density at

which LTE will hold absolutely. Furthermore, doubt is cast on the reliability of LTE diagnostic techniques, and on the values of plasma properties calculated based on an LTE plasma composition. For these reasons non-LTE diagnostic techniques are called for in laser sustained plasmas, with the outcome of the interacting plasma processes being determined without bias. In addition values for the coefficients which determine laser energy absorption and plasma radiative emission can be calculated based on these unbiased measurements, resulting in a more accurate evaluation of plasma performance.

3. Maxwellian Electron Velocity Distribution

All of the above analysis hinges on the assumption that the electron velocity distribution is Maxwellian. This can be shown to be the case in LSP's by applying a criterion given by Langdon [33];

$$\frac{Zv_o^2}{v_e^2} \geq 1$$

When this inequality is satisfied, inverse bremsstrahlung absorption of laser radiation results in a non-Maxwellian velocity distribution. In this inequality Z is the ionic charge, v_o is the peak velocity of oscillation of the electrons in the high frequency electric field, and v_e is the electron thermal velocity. The above ratio may be expressed as;

$$\frac{Zv_o^2}{v_e^2} = (4 \times 10^{-16}) \frac{Z I \lambda^2}{T_e}$$

where I is the laser irradiance in W/cm^2 , λ is the laser wavelength in microns, and T_e is the electron temperature in keV. For a singly ionized gas at 1 eV, laser irradiance of $10^6 W/cm^2$, and a wavelength of 10.6 microns this parameter has a very small value. Therefore it can safely be concluded that the electron velocity distribution in laboratory LSP's is Maxwellian.

C. Laser Absorption and Radiative Emission in LSP's

In this section absorption and emission coefficients applied to LSP's will be discussed. The various coefficients will be examined in a non-LTE context and their validity for use in this proposed research determined.

1. Absorption Coefficients

The absorption of laser radiation in an LSP is the result of several important processes. At the laser wavelength of interest in this proposal, 10.6 microns, electron-ion IB is the dominant process [34]. At intermediate temperatures near 10,000 K electron-neutral IB becomes competitive due to the lower degree of ionization. Photoionization accounts for a significant fraction of the absorption at intermediate temperatures, but the overall absorption due to ionization is much greater at high temperature (15,000 K-20,000 K).

The two IB processes are called free-free meaning that an electron in a free state absorbs a photon in the presence of an ion or neutral atom and is accelerated into a more energetic free state. For the electron-ion IB this process is essentially independent of the heavy particle species as long as the electron can be considered moving in a Coulomb field. The absorption coefficient for argon can then be found from the expression derived for hydrogen. The laser absorption for any given species then depends on the actual plasma composition.

Photoionization is a bound-free process in which an electron bound to an atom absorbs a photon of sufficient energy to elevate it to a free state. This process is also independent of the atomic structure as long as the photons do not have sufficient energy to free electrons from bound levels below the merged level limit [35]. This condition is satisfied for the long laser wavelength and electron number densities expected in this proposed research. The absorption coefficients for electron-ion IB and photoionization are often combined in the form [35];

$$K_{ei} + K_p = (1.37 \times 10^{-23}) z n_e^2 \frac{\lambda^3}{\sqrt{T}} \left[1 - \exp\left[\frac{-hv}{kT}\right] \right] h_\lambda(n_e, T) g(\lambda, T)$$

where $g(\lambda, T)$ is the free-free Gaunt factor accounting for a nonhydrogenic quantum mechanical correction, and h_λ is a factor accounting for the photoionization. For the case of long wavelength h_λ is given by [35];

$$h_\lambda(n_e, T) = \exp\left[\frac{hv}{kT}\right]$$

All quantities should be expressed in the cgs-esu system. The factor z accounts for the ionic charge of argon being greater than unity at higher temperatures where second ionization occurs.

This correction is roughly equal to unity until the temperature increases past 20,000 K. The first bracketed term accounts for the stimulated reemission of absorbed laser energy.

The laser absorption due to electron-neutral IB does not enjoy the convenience of particle species independence. The absence of a dominant Coulomb field renders the absorption rate dependent upon short range interactions. According to Geltman [36], in this case analytical approximations are unavailable and calculations must be performed numerically. In Geltman's calculations it is assumed that the atom can be represented by a spherically symmetric potential which depends on the atoms ground state structure. A total free-free absorption cross section is calculated and used to determine a mean absorption coefficient averaged over the electron thermal energy distribution. Geltman gives results for numerous gases including argon for wavelengths 0.5 μm -20 μm and electron temperatures 500 K-20000 K. From these data a curve fit has been applied, resulting in the following for the IB absorption of 10.6 μm radiation by neutral argon;

$$K_{\text{en}}(T) = 10^{\left[2.2738 \log(T) - 45.124\right]} \left[1 - \exp\left[\frac{-h\nu}{kT}\right]\right] n_e n_a$$

In a non-LTE situation, all of the absorption coefficients presented can be used as is. This is because the relevant temperature in each case is the free electron temperature. It should be noted that for situations in which the bound-free absorption is not initiated above the merged level limit, e.g. for short laser wavelengths, then this would not be the case and level populations would be a factor. Fortunately this is not the case for the laser wavelength in this proposed research. Also, the contributions from excited states to the electron-neutral IB have been approximated by the ground state result. Because the excitation of argon is small at the temperatures at which electron-neutral IB is important, this approximation should not induce much error in any case.

The significant non-LTE effect on laser absorption will be in applying actual plasma constituent densities into the coefficient expressions. Most tabulated absorption coefficient data assumes a Saha equilibrium composition at the electron temperature. In this research measured and/or calculated values of the particle densities will be applied in conjunction with a calculated electron temperature to arrive at non-LTE absorption coefficients.

2. Emission Coefficient

In previous investigations of argon LSP's [12-14] the derivation of Kozlov et al. [37] was used to calculate the total emissive power of an argon plasma;

$$\epsilon_v = 5.44 \times 10^{-39} \frac{n_e n_i}{\sqrt{T}} \exp\left[\frac{-\Delta I}{kT}\right] \xi(v) \exp\left[\frac{h(v_g - v)}{kT}\right]$$

As before all values are to be in cgs-esu units. ΔI is the lowering of the ionization potential and can be calculated according to Griem [32, p.139], v_g is the maximum photoelectric threshold frequency corresponding to the series limit, and $\xi(v)$ is a factor which takes into account the structure of the contributing atomic levels.

The above expression accounts for free-free, free-bound, and bound-bound emissive power. This expression is actually a modification of the Biberman-Norman continuum expression accounting for only bremsstrahlung and recombination [38]. The modification lies in the assuming that all the levels in argon except the 4s levels can be represented by a continuous sequence. Therefore v_g now corresponds to the lowest lying 4p level 2.85 eV below the ionization potential of argon. In this way the contribution of the entire line spectrum (except for the 4s levels) to the spectral emissive power is approximately taken into account. Kozlov asserts that the "smearing out" of discrete lines in this manner is of little significance in optically thin plasmas because the end result will involve an integration over the spectrum.

The integration over all frequencies is simplified if the assumption $\xi(v)=1$ is made. This is a good approximation at the low frequencies at which the exponential factor will be large [37], so that the integration gives;

$$\int_0^{\infty} \xi(v) \exp\left[\frac{-hv}{kT}\right] dv = \frac{kT}{h}$$

and for the total emissive power;

$$\epsilon_s = \int_0^{\infty} \epsilon_v dv = 1.14 \times 10^{-28} n_e n_i \sqrt{T} \exp\left[\frac{hv_g - \Delta I}{kT}\right]$$

where the units are W/cm³ sr.

This formula is basically an approximation and does not include the contribution due to the 4s levels. Fortunately, for argon Kozlov states that this omission is almost completely compensated for by the overestimate in the emissive power in the region of small quanta. This is because near the 4p level, transitions with small quanta are impossible due to the 1 eV gap separating these levels from the next higher lying group.

Kozlov concludes by comparing calculations based on the above expression to integrated emissive power data from experiments using an argon plasma. The calculations were performed assuming an equilibrium composition and the agreement seems to be very good.

Due to the assumptions included in the derivation of this expression, there is no dependence on the atomic structure except for in the selection of ν_g . The excited state distribution temperature does not enter into the formulation and the electron temperature remains as the relevant parameter. As in the case of the laser absorption coefficient, any non-LTE effect will be manifested in the actual plasma constituent densities to be used in the emissive power expression.

III. Experimental and Analytical Techniques

In this section the proposed experimental and analytical techniques for determining the thermodynamic state of a non-LTE laser sustained plasma will be discussed. Stark broadened line profiles and excited state populations will be measured experimentally, and an analytical algorithm used to determine other relevant parameters such as electron temperature and number density, heavy particle temperature, neutral particle number density, and total excitation temperature.

A. Experimental Techniques

1. Electron Number Density

The method of Stark broadening of the $H\beta$ line will be used in measuring the electron number density. For this purpose a small amount of hydrogen will be added to the argon before it enters into the plasma chamber. Adding <1% hydrogen by volume is not expected to greatly effect the state of the plasma [39]. Stark broadened profiles of the $H\beta$ line have been calculated by Vidal et al. [40] from which the electron number density can be determined from measured profiles. A correction scale for this determination has been given by Baessler and Kock [41] based on

interferometric measurements of electron number density. The profiles have a slight temperature dependence which can be handled in the analytical scheme described in the next section.

The distribution of electron number density in an LSP is expected to be inhomogeneous. Therefore the measured line-of sight spectral intensities in the $H\beta$ line must be inverted with the Abel transform to give point spectral emissivities [42]. The measured profile must be divided into a reasonable number of strips, to each of which the Abel transformation is applied. The resulting array of emissivities can then be transposed to reconstruct the line profile at each point in the plasma. In addition the effects of self-absorption, instrument broadening, and Doppler broadening must be considered in order to assure accurate values [32].

2. Absolute Line Intensity

The measurement of absolute line intensities will be used to determine the upper level state populations in neutral argon. An Abel inversion of the calibrated (standard technique) net line intensity must be performed to obtain the line emission coefficient. From this the state populations of the upper levels of the line transitions can be found from;

$$n_m = \left[\frac{4\pi}{h\nu} \right] \frac{i_L}{A_{mn}}$$

where $h\nu$ is the energy of the transition, A_{mn} is the spontaneous transition rate, and i_L is the line emission coefficient (W/cm^3sr). From these the upper level excitation temperature, denoted $T_{ex\beta}$ by Eddy [43], can be determined from the Boltzmann factors;

$$\frac{n_m}{g_m} = \frac{n_n}{g_n} \exp \left[\frac{-(E_m - E_n)}{kT_{ex\beta}} \right]$$

where the E 's and g 's are the energy levels and degeneracies of the states involved. Several well spaced optically thin (or absorption corrected) lines used in this manner should result in a linear Boltzmann plot which can be extrapolated to the lowered ionization limit to determine the population of the highest excited state, n_I , which will be important in the analytical solution. There is some discrepancy over the values of the transition rates in argon [44] and suitable values must be located in order to assure the accuracy of these measurements.

B. Analytical Techniques

Following the work of Eddy et al.[18,19] an algorithm will be developed which uses measured values from the Stark profiles of the H β line, the highest excited state population, and the chamber pressure. The results of the calculation should yield the electron number density $n_e=n_i$, electron temperature T_e , heavy particle temperature $T_a=T_i$, neutral particle number density n_a , and the total excitation temperature T_{exa} which relates the ground state population and n_a to the known population of the highest excited state. Hence the known quantities are n_I/g_I , pressure, and the Stark profile. There are five unknowns as listed above and so five relations are needed to achieve a solution. The first comes from the Stark profile calculations of Vidal et al. which require electron temperature to arrive at n_e . Three of the four remaining equations are taken from Eddy et al. and are as follows;

The total Boltzmann distribution:

$$\frac{n_a}{Z_{\text{exa}}} = \frac{n_I}{g_I} = \frac{n_I}{g_I} \exp\left[\frac{-E_{I,a}}{kT_{\text{exa}}}\right]$$

The Generalized Multithermal Equilibrium (GMTE) highest level ionization equation:

$$n_e \left[\frac{n_i}{n_I} \right]^{\frac{T_g}{T_e}} = 2 \left[\frac{Z_{\text{exa}}}{g_I} \right]^{\frac{T_g}{T_e}} \left[\frac{Z_{\text{exi}}}{Z_{\text{exa}}} \right]^{\frac{T_{\text{exa}}}{T_e}} \left[\frac{2\pi m_e k T_e}{h^2} \right]^{\frac{3}{2}} \exp\left[\left[\frac{-E_{I,a}}{kT_e} \right] \left[\frac{(T_{\text{exa}} - T_g)}{T_{\text{exa}}} \right] \right]$$

The equation of state:

$$p = n_e k T_e + (n_a + n_i) k T_g$$

Several equations may be attempted for the last required relation. Among the possibilities are the electron or heavy particle energy equations, which require thermophysical and transport properties, absorption and emission equations, and some knowledge of the macroscopic velocity field. It is in the choice of this last relation that the success of the solution scheme hinges and a strong effort must be made in this regard.

Once a set of equations is decided upon, an iterative scheme initialized with LTE values based on the excited state populations can be implemented to determine all unknown quantities.

C. Proposed Experimental Agenda

The first experiments will deal with argon plasmas in the operating regimes already mapped out by conventional diagnostic techniques, spectroscopic and otherwise. Laser power will range up to 7 kW at gas pressures of 1 atm. and 2.5 atm. Gas mass flux will range throughout the entire stability regime the plasmas, and two beam focusing geometries are possible. These experiments will provide information on the equilibrium state of the plasmas that have been observed in previous work, and provide better values for absorption coefficient and emissive power of the plasma. Comparisons will be made to the previous results concerning temperature distributions, global absorption, and thermal conversion efficiency.

In the event that non-LTE does persist in these LSP's, the next series of experiments will be aimed at determining conditions under which LTE can be fully expected. It is thought that elevated pressures will be required to achieve the electron number densities necessary for this occurrence.

IV. References

- [1] Kantrowitz, A. R., "The Relevance of Space," *Astronautics and Aeronautics*, Vol. 9, p. 34, 1971.
- [2] Kantrowitz, A. R., "Propulsion to Orbit by Ground-Based Lasers," *Astronautics and Aeronautics*, Vol. 10, p. 74, 1972.
- [3] Glumb, R. J. and Krier, H., "Concepts and Status of Laser-Supported Rocket Propulsion," *Journal of Spacecraft and Rockets*, Vol. 21, p. 70, 1984.
- [4] McMillin, B. K., Energy Conversion in Laser Sustained Argon Plasmas for Application to Rocket Propulsion, M.S. Thesis, University of Illinois at Urbana-Champaign, 1987.
- [5] Zerkle, D. K., Schwartz, S., Mertogul, A., Chen, X., Krier, H., and Mazumder, J., "Laser-Sustained Argon Plasmas for Thermal Rocket Propulsion," to appear in the *Journal of Propulsion and Power*, Jan.-Feb. 1990.
- [6] Mertogul, A. E., Energy Absorption and Thermal Conversion Efficiency in Argon Laser Sustained Plasmas, M.S. Thesis, University of Illinois at Urbana-Champaign, 1989.
- [7] Schwartz, S., Mertogul, A., Eguiguren, J., Zerkle, D., Chen, X., Krier, H., and Mazumder, J., "Laser-Sustained Gas Plasmas for Application to Rocket Propulsion," AIAA Paper 89-2631, AIAA/ASME/SAE/ASEE 25th Joint Propulsion Conference, July 1989.
- [8] Dresvin, S. V., Physics and Technology of Low-Temperature Plasmas, p. 77, Iowa State University Press, Ames, Iowa, 1977.
- [9] Biberman, L. M., Vorob'ev, V. S., and Yakubov, I. T., Kinetics of Nonequilibrium Low-Temperature Plasmas, Consultants Bureau, New York, 1987.
- [10] Generalov, N. A., Zimakov, V. P., Kozlov, G. I., Masyukov, V. A., and Raizer, Y. P., "Experimental Investigation of a Continuous Optical Discharge," *Soviet Physics-JETP*, Vol. 34, p. 763, 1972.
- [11] Kozlov, G. I., Kuznetsov, V. A., and Masyukov, V. A., "Sustained Optical Discharges in Molecular Gases," *Soviet Physics-Technical Physics*, Vol. 49, p. 1283, 1979.
- [12] Welle, R., Keefer, D., and Peters, C., "Laser-Sustained Plasmas in Forced Argon Convective Flow, Part I: Experimental Studies," *AIAA Journal*, Vol. 25, No. 8, p. 1093, 1987.
- [13] Glumb, R. J., and Krier, H., "Two-Dimensional Model of Laser-Sustained Plasmas in Axisymmetric Flowfields," *AIAA Journal*, Vol. 24, No. 8, p. 1331, 1986.
- [14] Jeng, S.-M., and Keefer, D. R., "Theoretical Investigation of Laser-Sustained Argon Plasmas," *Journal of Applied Physics*, Vol. 60, No. 7, 1986.
- [15] Mazumder, J., Rockstroh, T. J., and Krier, H., "Spectroscopic Studies of Plasma During CW Laser Gas Heating in Flowing Argon," *Journal of Applied Physics*, Vol. 62, No. 12, p. 4712, 1987.
- [16] Eguiguren, J. V., A Steady Two-Dimensional Flow Model for Laser Sustained Plasmas, M.S. Thesis, University of Illinois at Urbana-Champaign, 1989.

- [17] Eddy, T. L., "Critical Review of Plasma Spectroscopic Diagnostics via MTE," *IEEE Transactions on Plasma Science*, Vol. PS-4, No. 2, p. 103, 1976.
- [18] Eddy, T. L., and Sedghinasab, A., "The Type and Extent of Non-LTE in Argon Arcs at 0.1-10 Bar," *IEEE Transactions on Plasma Science*, Vol. 16, No. 4, p. 444, 1988.
- [19] Eddy, T. L., "Low Pressure Plasma Diagnostic Methods," AIAA Paper 89-2830, AIAA/ASME/SAE/ASEE 25th Joint Propulsion Conference, July 1989.
- [20] Keefer, D. R., Henriksen, B. B., Braerman, W. F., "Experimental Study of a Stationary Laser-Sustained Air Plasma," *Journal of Applied Physics*, Vol. 46, No. 3, p. 1080, 1975.
- [21] Cremers, D. A., Archuleta, F. L., and Martinez, R. J., "Evaluation of the Continuous Optical Discharge for Spectrochemical Analysis," *Spectrochimica Acta*, Vol. 40B, No. 4, p. 665, 1985.
- [22] Rachman, A., and Bassani, L., "Local Thermodynamic Equilibrium Conditions in Superhigh-Pressure Helium Plasmas Produced by Laser Action," *Physical Review Letters*, Vol. 23, No. 17, p. 954, 1969.
- [23] Tonon, G., Schirman, D., Rabeau, M., "Electron and Ion Temperature Measurements of a Laser Created Plasma,"
- [24] Vorob'ev, V. S., and Khomkin, A. L., "Thresholds for the Appearance of Various States of a Nonequilibrium-Ionization Plasma Produced Near a Metal Surface by Laser Bombardment," *Soviet Technical Physics Letters*, Vol. 10, No. 8, p. 399, 1984.
- [25] Farmer, A. J. D., Haddad, G. N., "Local Thermodynamic Equilibrium in Free-Burning Arcs in Argon," *Applied Physics Letters*, Vol. 45, No. 1, p. 24, 1984.
- [26] Bober, L., Tankin, R. S., "Investigation of Equilibrium in an Argon Plasma," *Journal of Quantitative Spectroscopy and Radiative Transfer*, Vol. 10, p. 991, 1970.
- [27] Freeman, M. P., "A Quantitative Examination of the LTE Condition in the Effluent of an Atmospheric Pressure Argon Plasma Jet," *Journal of Quantitative Spectroscopy and Radiative Transfer*, Vol. 8, p. 435, 1968.
- [28] Simon, D. R., and Rogers, K. C., "Spectroscopic Investigations of the Helium Short Arc," *Journal of Applied Physics*, Vol. 37, No. 6, p. 2255, 1966.
- [29] Kruger, C. H., "Nonequilibrium in Confined-Arc Plasmas," *The Physics of Fluids*, Vol. 13, No. 7, p. 1737, 1970.
- [30] Uhlenbusch, J. F., and Fischer, E., "Influence of Diffusion and Nonequilibrium Populations on Noble-Gas Plasmas in Electric Arcs," *Proceedings of the IEEE*, Vol. 59, No. 4, 1971.
- [31] Giannaris, R. J., and Incropera, F. P., "Nonequilibrium Effects in an Atmospheric Argon Arc Plasma," *Journal of Quantitative Spectroscopy and Radiative Transfer*, Vol. 11, p. 291, 1971.
- [32] Griem, H. R., *Plasma Spectroscopy*, p. 131, McGraw-Hill, New York, 1964.
- [33] Langdon, A. B., "Nonlinear Inverse Bremsstrahlung and Heated-Electron Distributions", *Physical Review Letters*, Vol. 44, No. 9, p. 575, March 3, 1980.

- [34] Stallcop, J. R., "Absorption of Laser Radiation in a H-He Plasma. I. Theoretical Calculation of the Absorption Coefficient", *The Physics of Fluids*, Vol. 17, No. 4, p. 751, April 1974.
- [35] Stallcop, J. R., "Absorption Coefficients of a Hydrogen Plasma for Laser Radiation", *Journal of Plasma Physics*, Vol. 11, Part 1, pp. 111, 1974.
- [36] Geltman, S., "Free-Free Radiation in Electron-Neutral Atom Collisions", *Journal of Quantitative Spectroscopy and Radiative Transfer*, Vol. 13, pp. 601, 1973.
- [37] Kozlov, G. I., Kuznetsov, V. A., and Masyukov, V. A., "Radiative Losses by Argon Plasma and the Emissive Model of a Continuous Optical Discharge", *Soviet Physics-JETP*, Vol. 39, No. 3, p. 463, September 1974.
- [38] Biberman, L. M., and Norman, G. É., "Continuous Spectra of Atomic Gases and Plasma", *Soviet Physics Uspekhi*, Vol. 10, No. 1, p. 52, July-August 1967.
- [39] Eddy, T. L., Personal Communication.
- [40] Vidal, C. R., Cooper, J., and Smith, E. W., "Hydrogen Stark-Broadening Tables", *The Astrophysical Journal Supplement Series No. 214*, Vol. 25, p. 37, 1973.
- [41] Baessler, P., and Kock, M., "An Interferometric and Spectroscopic Study on a High-Current Argon Arc", *Journal of Physics B*, Vol. 13, p. 1351, 1980.
- [42] Cremers, C. J., and Birkebak, R. C., "Application of the Abel Integral Equation to Spectrographic Data," *Applied Optics*, Vol. 5, p. 1057, 1966.
- [43] Eddy, T. L., Ph.D. Thesis, University of Minnesota, 1972.
- [44] Sedghinasab, A., Ph.D. Thesis, Georgia Institute of Technology, 1987.

APPENDIX A

MICROTEX DIGITAL IMAGING SYSTEM

Many of the modern laser diagnostic techniques presently applied to spectroscopic flow visualization studies produce low intensity light images. Such is the case for the PLIF (planar laser induced fluorescence) technique that will be applied to the scramjet combustion experiments. Another inherent difficulty in analyzing such a phenomenon, especially in a high speed flow, is achieving reasonably high spatial and temporal resolution. A very fine temporal resolution can significantly contribute to a reduction in the intensity of the light available to be captured. The Microtex imaging system offers high resolution image intensification and high speed, solid-state digital subsystems for data acquisition and also the flexibility of image processing and display. The basic system hardware components consist of a DEC MicroVax II minicomputer that serves as the control center, a separate DEC PDP-11 shell that contains an ultra-fast (5 MHz) analog/digital converter and high-speed memory boards, an Omnicomp graphics display processor, a Summagraphics digitizing tablet, a Barco high resolution 1280 x 1024 color monitor, a Microtex pulse power supply, and an intensified 128 x 128 photodiode array Reticon camera.

Image Acquisition

Bypassing the details of any particular laser diagnostic technique, two of the most crucial aspects of image acquisition are the speed of data capture and the ability to detect low levels of light. The image acquisition speed is limited, not by the camera (which can read out data at a pixel rate of up to 8 Mhz), but by the 12 bit A/D converter which can accept and decode a 128 x 128 pixel image in approximately 4 milliseconds. Considering the time required for data transfer into memory and other factors, the maximum frame rate is set at approximately 220 full frames per second. Since partial frames (as small as 128 x 2 pixels) can be taken, framing rates of over 1,000 frames per second for essentially a one-dimensional linear array are possible.

The image acquisition is accomplished via an intensified solid-state camera (or a normal, unintensified camera if the intensity of the light is adequate) that consists of a 128 x 128 photo-diode array. The array is a square, 7.7 mm on a side, corresponding to approximately 8 lp/mm spatial resolution (or 60 microns between pixel centers). The image intensifier can be thought of as an amplifier of photons, a device that produces an output that is an intensified replica of the input image. A conceptual sketch of the intensified camera is shown in Figure 1.

Incoming photons strike the photocathode and are absorbed and converted into electrons, often referred to as photoelectrons. These photoelectrons are then accelerated by a voltage potential and enter the microchannel plate (MCP); this is where the actual intensification occurs. The MCP is basically a bundle of microscopic hollow tubes whose insides have been coated with a dynode-type material and work in a manner similar to a photo-multiplier. A dynode is a surface consisting of material that will readily give up additional electrons when excited by the energy of an incident electron. Photoelectrons from the cathode travel down through these tubes ricocheting off the sides and releasing additional electrons along the way; hence producing the amplification effect.

These electrons are further accelerated by an additional voltage potential and then converted back into photons upon striking the back of the aluminum plate and exciting a phosphor coating on the other side. The phosphor molecules are energized into a higher quantum state and release photons upon decay. The intensified image is reduced in size by a fiber-optic minifier and then captured by the photodiode array. Fiber-optic coupling is far more efficient than lens coupling and therefore makes optimal use of the gain produced by the intensifier. Figure 2 shows a grayscale version of a bunsen burner flame image that was taken with an unintensified camera. Figure 3 is an image of a propane torch flame that was taken with the intensified camera at an effective shutter speed of 1/2000 using a 55 mm Nikkor lens set at f/11.

Image Processing

The Microtex software affords a wide range of image processing functions, some of which are addition, subtraction, multiplication and division of any two image arrays. For example, it may be desirable to separate the background noise from the intended intensity/temperature data from PLIF. An image of the flowfield, less the fluorescence generated by the pulsed laser sheet, could be taken, then subtracted from the PLIF image. Other functions include Laplace, gradient, convolution, log base ten, natural log, square root, derivative in the x direction or y direction, and high or low pass filters.

Analysis of the image is another attribute of the system. The measuring capabilities of the system can give a pixel to pixel account of positions and intensities of a camera image. High and low values of intensities can be found along with their spatial location. The median of the intensities over an entire image can be found and even a histogram of any line through the image can be generated. Microtex software also permits plotting of the camera image data in a number of insightful configurations. In addition to displaying the actual image, the data can be represented as three dimensional graphs, two dimensional contours, and slice maps that all give excellent visual interpretations of the data for quantitative analysis. Through our own software modifications we can convert ordinary text format data into Microtex image format data and render them as a pseudo-camera image; as is the case in Figures 4, 5 and 6 for heat exchanger data generated from a computer model. Another illustration of this process is a gaussian distribution data image shown in Figure 7 as a 3-D contour with a ceiling. These hard copies were generated by converting the colors on the Microtex system into corresponding grayscale values, down-loading to the Macintosh, and then printing the results on an Apple laserwriter.

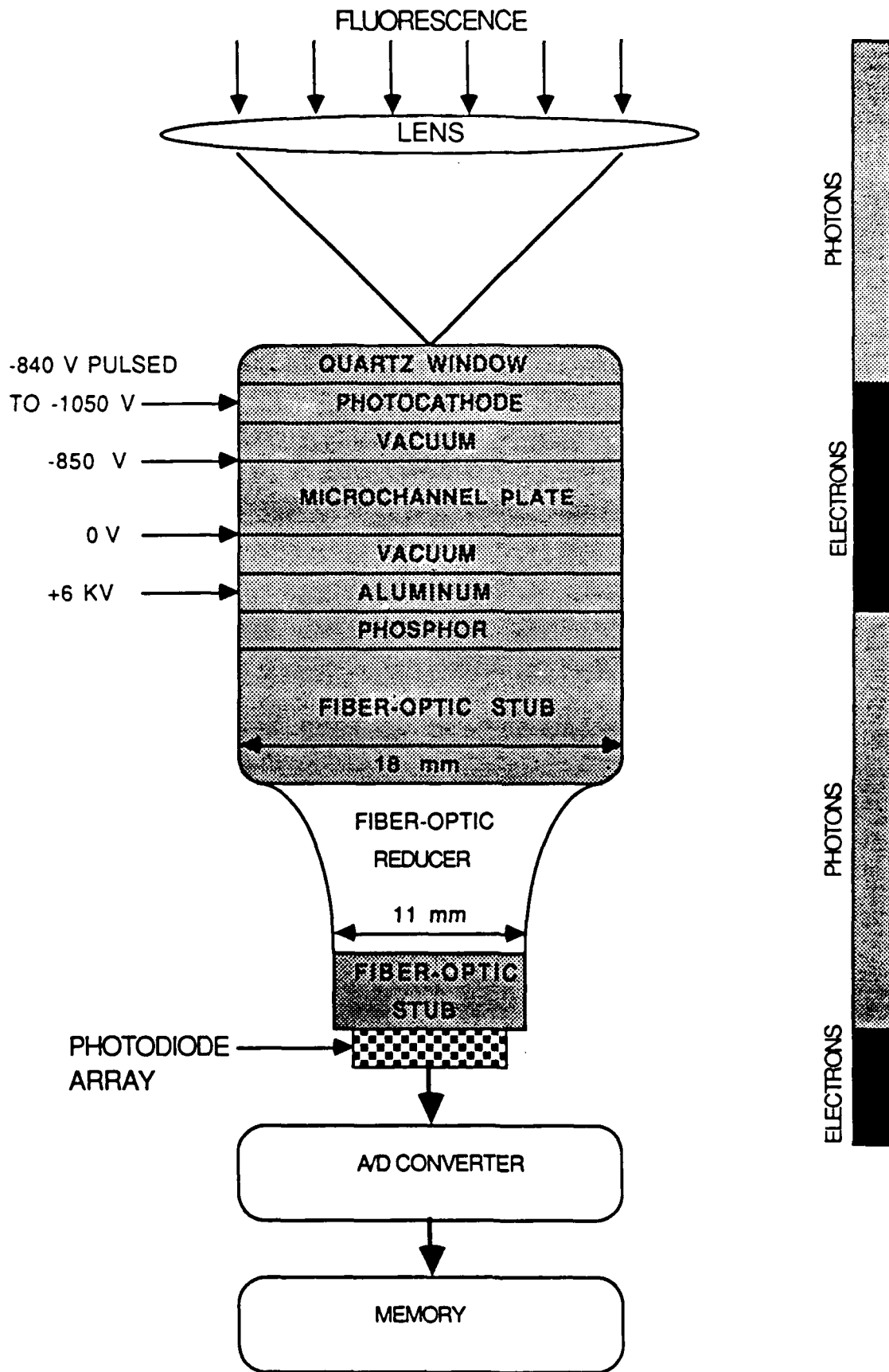
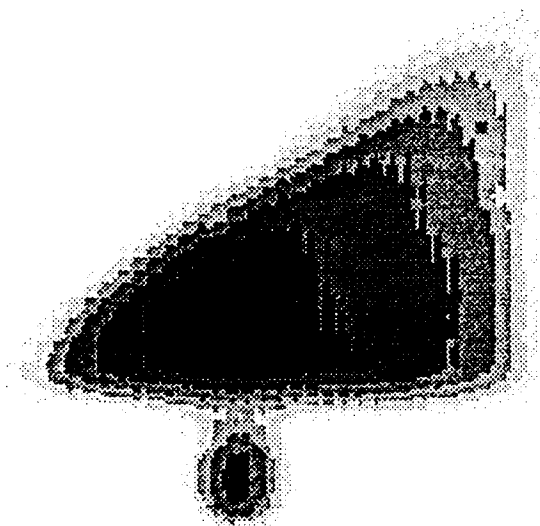


FIGURE 1. INTENSIFIED CAMERA



=	0	to	156
=	156	to	312
=	312	to	468
░░░	=	468	to 624
▒▒▒	=	624	to 780
▓▓▓	=	780	to 936
■	=	936	to 1092
■	=	1092	to 1248

Figure 2.

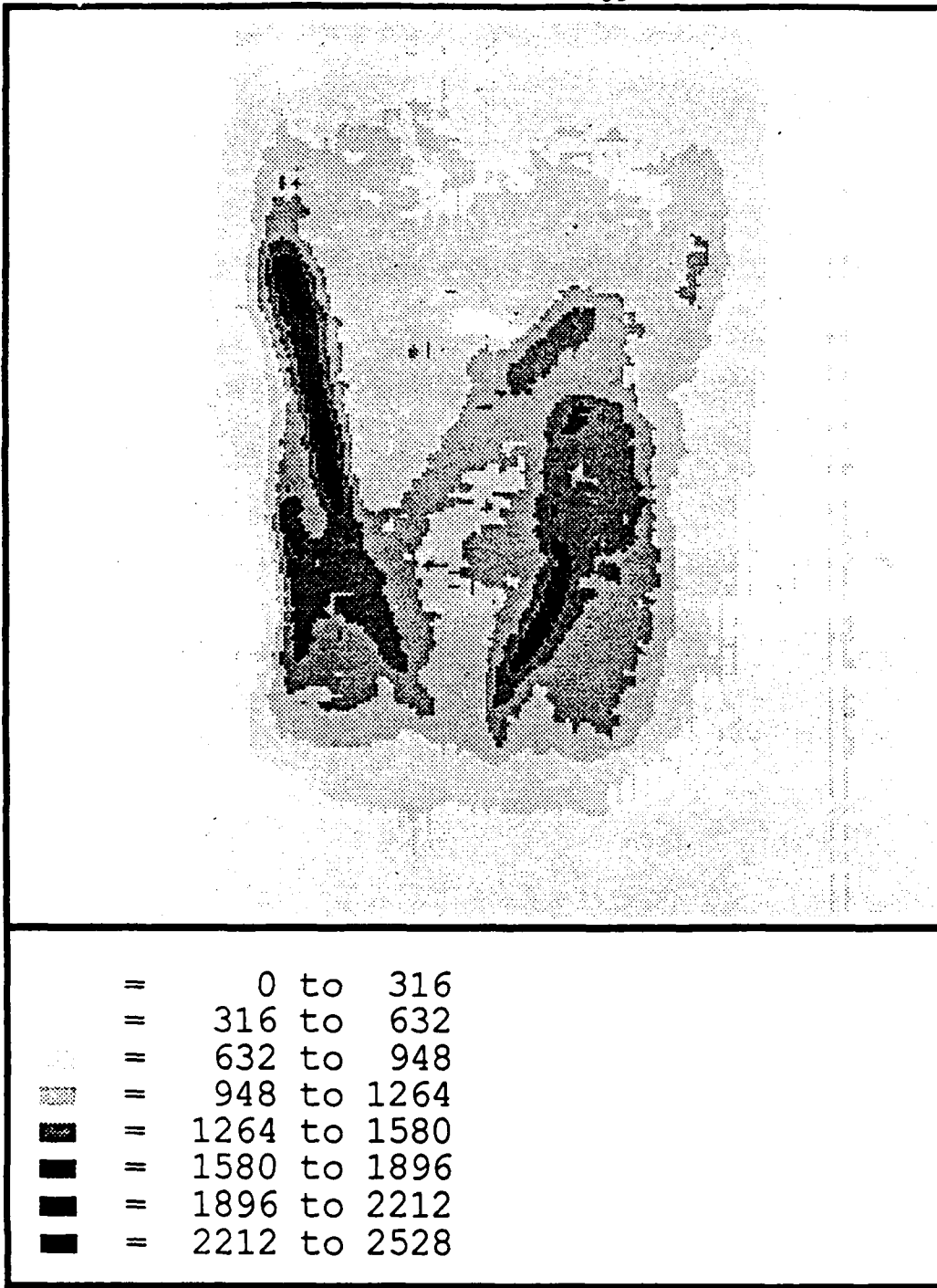


Figure 3.

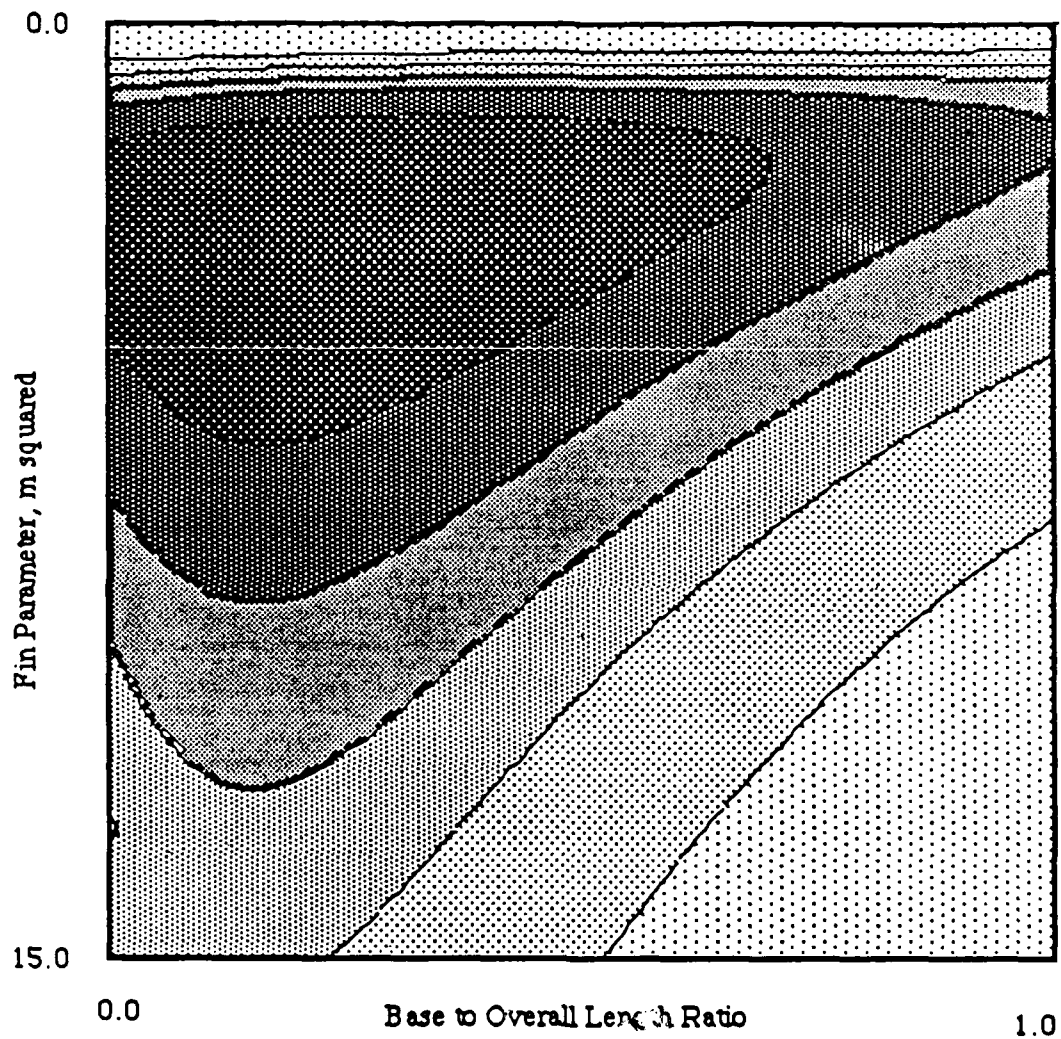


Figure 4.

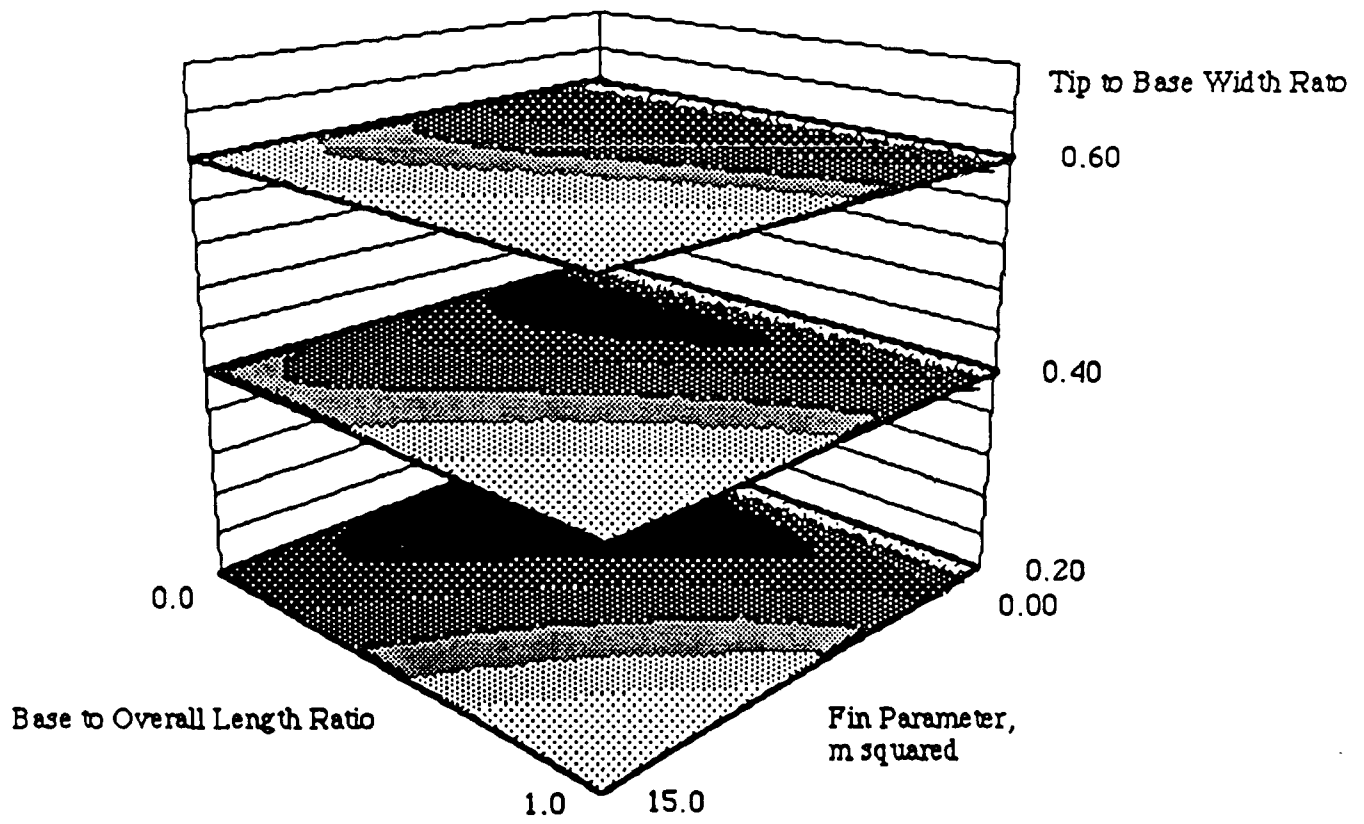


Figure 5.

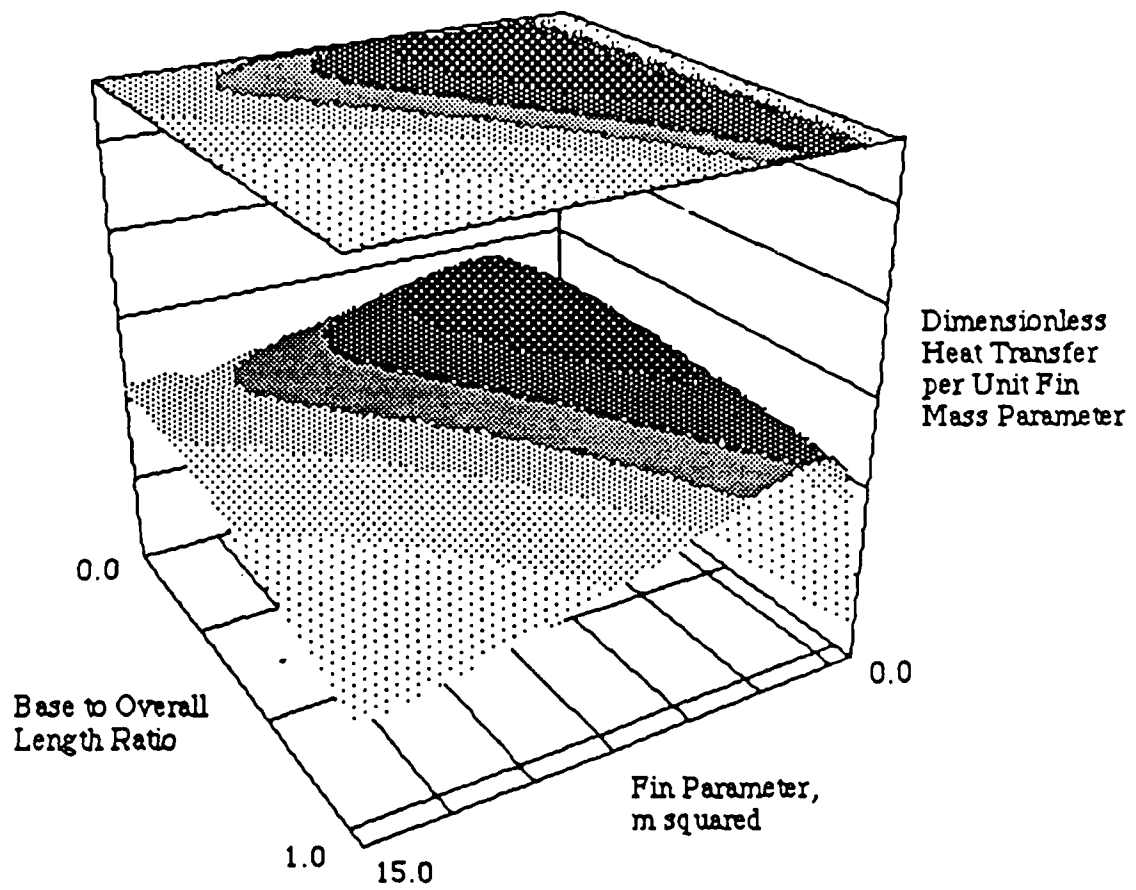


Figure 6.

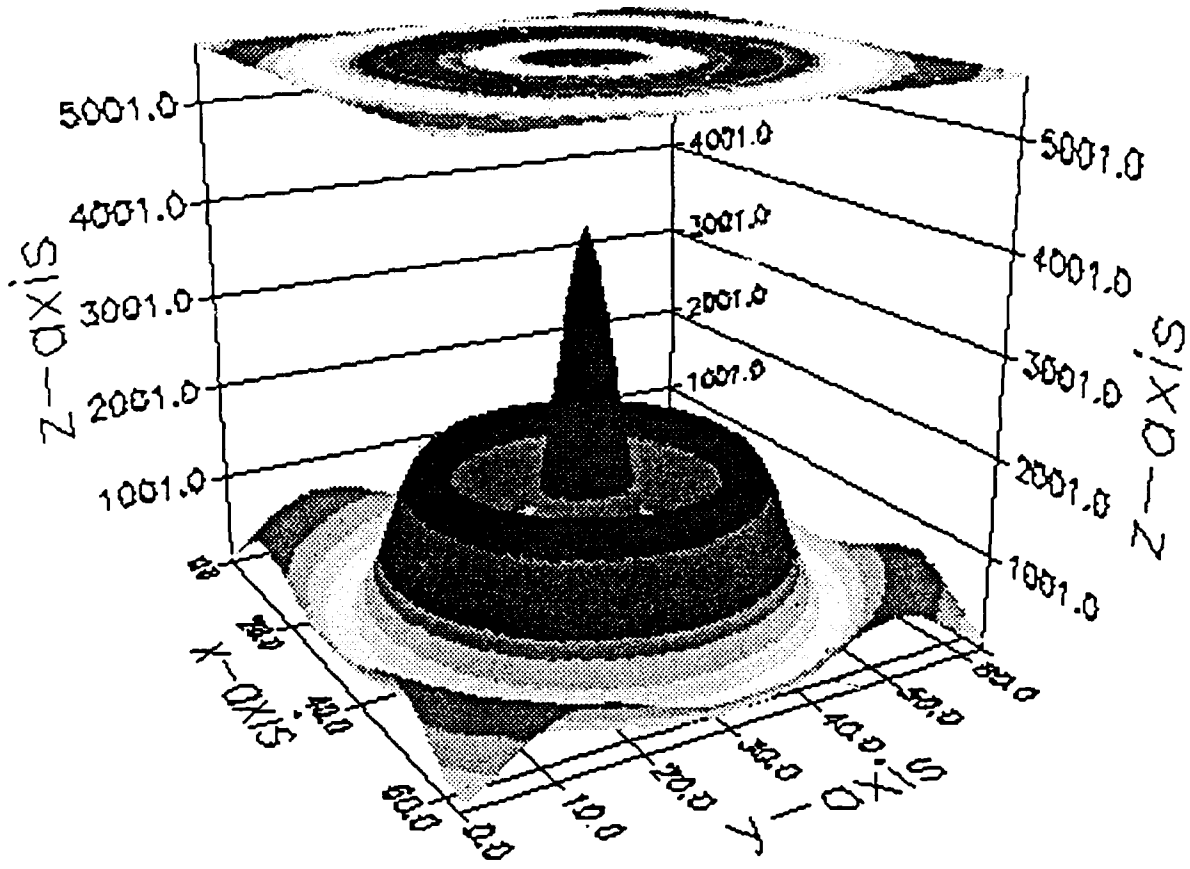


Figure 7.

APPENDIX B

LASER-INDUCED FLUORESCENCE

Of the most popular advanced combustion diagnostics, Raman fluorescence is characterized by very low signal levels, thus limiting its utility to major species in combustion systems. Laser-Induced Fluorescence (LIF), however, has signal strengths several orders of magnitude greater than Raman methods without as much complexity as Coherent Anti-Stokes Raman Spectroscopy (CARS), which is by far the most intricate and involved system [1]. With the capacity to trace certain regions of a combustion zone via short lived radical species, LIF was chosen as the method with which to map combustion temperatures as well as species transport of the reaction zone.

Until recently, LIF studies dealt mainly with flames, since the flame radicals of interest could be excited with conventional lasers and optical doubling techniques. Due to recent advances in multiphoton absorption with lasers operating in the ultraviolet, atomic flame species, namely O and H, heretofore inaccessible can now be investigated more readily [2,3]. In reactive flows, the most commonly investigated flame radical is the hydroxyl molecule, OH. This is primarily due the large amount of information regarding its molecular quantum structure and spectrum [4,5], but also due to the long fluorescence decay time and the abundance of OH in most combustion systems. Several other diatomic flame radicals are of particular interest, such as CH and CN, since they represent distinct regions of a combustion zone [6]. The classic inner cone structure of premixed burners is closely associated with CH emission within this hot, thin flame front region. The difficulty in investigating these molecules is that they are very short lived. Hydroxyl fluorescent lifetimes are on the order of several hundred nanoseconds while the CH and CN fluorescent decay are orders of magnitudes faster than for OH. Complications due to the complex rotational and vibrational structures of polyatomic flame species makes such radicals very difficult to probe. In contrast, atomic species have only electronic transitions, and the fluorescence techniques are typically easier to interpret.

For nonreactive flows, several LIF studies have illustrated the applicability of this diagnostic in supersonic flowfields. Several of the researchers have utilized the fluorescent strength of the sodium D line for investigation of high supersonic and hypersonic flows [8,9]. The sodium exhibited a Doppler shifted, pressure broadened absorption profile, allowing a narrow linewidth dye laser to be tuned to different frequencies within the broadband absorption profile, thereby causing regions of only a particular velocity component to fluoresce. Another study [10] used nitric oxide injected in known concentrations to measure the fluctuating temperatures in a supersonic boundary layer.

Absolute measurements of temperatures from fluorescence data is often clouded by unwanted collisional signal quenching. A method to overcome the spatial and specie variations of collisional cross section is to saturate the upper population states of the laser coupled energy levels. For typical combustion flame radicals, a high laser spectral intensity is required to provide the energy to approach saturation populations of the upper energy levels. This range lies between 10^6 to 10^9 W/cm²-cm⁻¹ for the primary flame radicals [11]. Recent improvements in lasers have enabled the viable range of saturation spectroscopy to be extended into the regime of planar imaging. Planar imaging is very useful in a qualitative sense, but absolute measurements in a combusting flow is limited by the survivability of suitable seedants in the harsh combustion environment. In this sense, saturation LIF can not only yield a two-dimensional picture of the flowfield, but also give rough absolute temperatures in a planar sheet, provided the variation of laser spectral intensity within the viewing region is small, and that the saturation threshold is achieved.

A flexible laser system for use in LIF studies is generally comprised of a tunable dye laser pumped by either an excimer or a neodymium:yag laser. The key of the system is the dye laser, whose spectral range can be extended into the ultraviolet with the use of nonlinear optical doubling techniques. The pump laser, however, does play a significant role in the overall efficiency of the system. On the receiving aspect of fluorescence experiments is an intensified electronic camera for low intensity fluorescence detection.

The Scientific Imaging System from Microtex is ideally suited to this task, and consists of an intensified 128 x 128 pixel photodiode array camera, an image processor with a high resolution color monitor, and a gated pulse power supply, all built around a MicroVax II minicomputer.

The specifications of a flexible laser system highly depend upon the scope of activities planned for the lasers. An excimer laser operating with xenon chloride gas (XeCl @ 308 nm) can be used alone to provide broadband excitation of the nearby OH absorption band (306 nm) while also directly pumping a dye laser. A neodymium:yag laser (1.06 μm), however, must be tripled to approach the ultraviolet spectrum. Additionally, a XeCl excimer pumped dye laser has the widest range over all the traditional pumps, despite the efficiency being not quite as high. If flexibility is paramount, then the slight lack of efficiency can be overcome with a higher powered excimer, if this is necessary. Pulse to pulse repeatability of the energy level is very important in LIF, where variations in the laser intensity can greatly bias experimental results. The latest generation of commercial excimer lasers have options for maintaining a constant power output.

With the dye laser driven by the pump, if the output of the pump is constant, the output of the dye laser will also be very stable. The primary specification for a dye laser is the quality of the output beam in terms of linewidth. The standard dye laser cell employs an oscillator with a sine bar tuned moving grating. The spectral response is adequate, but a revolutionary oscillator design has appeared on the market in the Lumonics HyperDYE-300 series dye laser. Here the grating is fixed, and the cavity is closed with a precision optimized end mirror which is rotated to compensate for the grazing reflection angle change for different frequencies. With the grating fixed, operation is always in the zero order of the grating, resulting a constant spectral linewidth over the tuning range of the laser. This oscillator produces linewidths comparable to those found in etalon tuned dye lasers. A major accessory is a second harmonic generator (SHG) to extend the useful range of dye lasers into the ultraviolet. Many important combustion flame radicals fluoresce in the near

ultraviolet, making the SHG quite useful. In situations where the desired transitions are simply too far into the ultraviolet and atmospheric absorption is detrimental, the new technique is multiphoton excitation, where the excitation wavelength is generally not as far into the ultraviolet so as to avoid some of the low wavelength problems.

Regarding saturation spectroscopy, the laser spectral intensity is defined as the power per pulse divided by the beam cross sectional area and by the frequency linewidth of the output beam. As mentioned above, the saturation threshold of the laser spectral intensity for various flame radicals is rather high. The linewidth is determined by the quality of the dye laser; hence a narrower linewidth enables attainment of saturation with lower overall power. With a dye laser and frequency doubler operating to deliver a beam at the hydroxyl transition of 306.4 nm, the typical overall efficiency at these wavelengths is roughly 2% that of the input pump beam on an energy/power basis. Thus saturation is more attainable with a system that has shorter pulse durations and a narrower dye output linewidth for a given input pulse energy.

With these laser properties and experimental constraints taken into account, the following is a list of the equipment slated for purchase, subject to the specifications listed thereafter. Of note is the request for a higher powered excimer than the low end models so that future studies in multiple wavelength excitation can be achieved by splitting the excimer and driving two dye lasers with only one pump laser.

REFERENCES

1. Bechtel, J.H. and A.R. Chraplyvy, "Laser Diagnostics of Flames, Combustion Products, and Sprays," Proceedings of the IEEE, Vol. 70, No. 5, pp. 658-677, 1982.
2. Hanson, R.K., "Combustion Diagnostics: Planar Imaging Techniques," presented at the 21st Symposium (International) on Combustion, Munich, West Germany, 1986.
3. Lee, M.P., P.H. Paul, and R.K. Hanson, "Laser-Fluorescence Imaging of O₂ in Combustion Flows using an ArF Laser," Optics Letters, Vol. 11, No. 1, pp. 7-9, 1986.
4. Dieke, G.H. and H.M. Crosswhite, "The Ultraviolet Bands of OH," Journal of Spectroscopic and Quantitative Radiation Transfer, Vol. 2, pp. 97-197, 1962.
5. Dimpfl, W.L. and J.L. Kinsey, "Radiative Lifetimes of OH(A ²Σ) and Einstein Coefficients for the A-X System of OH and OD," Journal of Quantitative Spectroscopy and Radiation Transfer, Vol. 21, pp. 233-241, 1979.
6. Bonczyk, P.A. and J.A. Shirley, "Measurement of CH and CN Concentration in Flames by Laser-Induced Saturated Fluorescence," Combustion and Flame, Vol. 34, pp. 253-264, 1979.
8. Miles, R.B., E. Udd, and M. Zimmermann, "Quantitative Flow Visualization in Sodium Vapor Seeded Hypersonic Helium," Applied Physics Letters, Vol. 32, No. 5, pp. 317-319, 1978.
9. Cheng, S., M. Zimmermann, and R.B. Miles, "Supersonic-Nitrogen Flow-Field Measurements with the Resonant Doppler Velocimeter," Applied Physics Letters, Vol. 34, pp. 253-264, 1979.
10. Gross, K.P. and R.L. McKenzie, "Measurement of Fluctuating Temperatures in a Supersonic Turbulent Flow Using Laser-Induced Fluorescence," AIAA Journal, Vol. 23, No. 12, pp. 1932-1936, 1985.
11. Eckbreth, A.C., P.A. Bonczyk, and J.F. Verdick, "Combustion Diagnostics by Laser Raman and Fluorescence Techniques," Progress in Energy and Combustion Science, Vol. 5, pp. 253-322, 1979.